https://rbgeomorfologia.org.br/
ISSN 2236-5664

Revista Brasileira de Geomorfologia

v. 24, nº 4 (2023)

http://dx.doi.org/10.20502/rbg.v24i4.2331

Research Article

Morphometric changes between Peroba and Redonda beaches (Ceará, Brazil), with the use of high resolution remotely piloted aircraft images from 2020 to 2021

Mudanças morfométricas entre as praias de Peroba e Redonda (Ceará, Brasil), com o uso de imagens de alta resolução obtidas por aeronave remotamente pilotada entre 2020 e 2021

Mário Silva Chacanza [1] Narelle Maia de Almeida [2] George Satander Sá Freire [3] Cláudio Ângelo da Silva Neto [4] Matheus Edson Mendes Medeiro [5] e João Capistrano de Abreu Neto [6]

[1] Federal University of Ceará, Programa de Pós-Graduação em Geologia, Laboratório de Geologia Marinha e Aplicada (LGMA), Fortaleza-Ceará, Brazil. Púnguè University (UniPúnguè), Tete City, Mozambique. mschacanza@gmail.com
ORCID: https://orcid.org/0000-0001-7679-1441

[2] Federal University of Ceará, Department of Geology, Programa de Pós-Graduação em Geologia, Laboratório de Geologia Marinha e Aplicada (LGMA), Fortaleza-Ceará, Brazil. narelle@ufc.br
ORCID: https://orcid.org/0000-0003-2586-4502

[3] Federal University of Ceará, Department of Geology, Programa de Pós-Graduação em Geologia, Laboratório de Geologia Marinha e Aplicada (LGMA), Fortaleza-Ceará, Brazil. satanderfreire@gmail.com
ORCID: https://orcid.org/0000-0001-8850-7225

[4] Federal University of Ceará, Programa de Pós-Graduação em Geologia, Laboratório de Geoprocessamento do Ceará (GEOCE), Fortaleza-Ceará, Brazil. claudioasn@gmail.com
ORCID: https://orcid.org/0000-0002-6749-9438

[5] Federal University of Ceará, Programa de Pós-Graduação em Geologia, Laboratório de Geologia Marinha e Aplicada (LGMA), Fortaleza-Ceará, Brazil. matheunh@gmail.com
ORCID: https://orcid.org/0000-0003-4496-4760

[6] Federal University of Ceará, Department of Geology, Laboratório de Geologia Marinha e Aplicada (LGMA), Fortaleza-Ceará, Brazil. joaoabreuneto@gmail.com
ORCID: https://orcid.org/0000-0002-4601-9386

Received: 10/12/2022; Accepted: 04/09/2023; Published: 30/10/2023

Abstract: Beaches are regions of the coastal zone where the effects of interaction between marine, terrestrial, and atmospheric ecosystems are often seen. Natural and anthropic agents act together in coastal processes, which may result in erosion or accretion. If the erosion is intense and continuous, it will represent a severe problem, especially in densely occupied and economically significant beaches, such as the beaches of Peroba and Redonda that have registered erosive events. Thus, this work aimed to analyze the variation of the coastline and the volume of beach sediments through a historical series of one year employing a remotely piloted aircraft, conjugated with the analysis of sediments collected in fields. At Peroba Beach, the shoreline was stable, having varied by about 0.87 m/year, and the volume indicated a positive sediment balance of about 18,815 m3. At Redonda Beach, the coastline degraded by about 1.27 m/year. The volume indicated a negative sediment balance of -1,230 m3. The beaches were mainly characterized by sediments of very fine and fine sand fractions. The volume variation indicated similar trends to the shoreline, with more significant deposition in the west and erosion in the east.

Keywords: Coastal erosion; Geoprocessing; Sediments; RPA.

Resumo: Praias são regiões da zona costeira onde os efeitos da interação entre os ecossistemas marinhos, terrestres e atmosféricos, são visualizados com frequência. Os agentes naturais e antrópicos atuam em conjunto nos processos costeiros, que podem resultar na erosão ou acreção. Se a erosão for intensa e contínua representará um grave problema, sobretudo em Praias densamente ocupadas e economicamente importantes, a exemplo das Praias de Peroba e Redonda que vem registrado eventos erosivos. Assim, este trabalho objetivou analisar a variação da linha de costa e o volume de sedimentos Praiais através de uma série histórica de um ano empregando uma aeronave remotamente pilotada, conjugada com análise de sedimentos coletados em campos. Na Praia de Peroba a linha de costa manteve-se estável, tendo variado cerca de 0,87 m/ano, o volume indicou um balanço positivo de sedimentos cerca de 18.815 m^3. Na Praia de Redonda a linha de costa progradou cerca de 1,27 m/ano, o volume indicou um balanço negativo de sedimentos na ordem de -1.230 m^3. As Praias foram caracterizadas majoritariamente por sedimentos de fração areia muito fino e fino. A variação de volume indicou tendências similares à da linha de costa, com maior deposição na porção oeste e erosão a leste.

Palavras-chave: Erosão costeira; Geoprocessamento; Sedimentos; RPA.

1. Introduction

Beaches are areas of the coastal zone that form an interface between the sea and the land, making them very dynamic regions because of the constant changes (SOUZA et al., 2005; MUEHE, 2013; KIM et al., 2018). Generally, beaches are composed of sandy sediments, making them very sensitive to topographic changes resulting from the direct action of wave energy, tides, currents, and anthropic activities, which may be reflected in erosive or depositional processes on the shoreline (KALIRAJ et al., 2017). The natural dynamics of coastal zones and anthropic actions potentiate the erosion problem and may result in topographic changes on different time scales (TAAOUATI et al., 2011; DEL RÍO et al., 2016; CHEN et al., 2018). Changes in terrain topography are always related to variations in the volume and granulometric characteristics of sediments that compose the beach. In this context, the granulometry of the sediment that composes a beach is extremely important for understanding the morphodynamic and hydrodynamic processes and the type of transport associated with its deposition (BARROS, 2018; QI et al., 2022).

Rapid surveys applying current technologies such as Remotely Piloted Aircraft (RPAs), popularly known as drones, have proved reasonably practical in coastal monitoring given their advantage in providing high temporal and spatial resolution geomorphological change data, besides the ease in creating aerophotogrammetric products, such as Digital Elevation Models (DEMs) and georeferenced orthophoto mosaics, when compared to data obtained from the traditional method based on satellite imagery and other approaches employing ground surveys (CASELLA et al., 2014; GOVAERE et al., 2016; CHEN et al., 2018; DAI et al., 2018; JANUŠAITĖ et al., 2019; JAUD et al., 2019, 2020; JAYSON-QUASHIGAH et al., 2019; PAGÁN et al., 2019; PITMAN et al., 2019). Repeated acquisitions of high-resolution DEMs allow for more accurate coastal monitoring, enabling the calculation of volumetric changes that occur over time, illustrating areas of erosion and sediment accretion as well as the land slope (BLANCHARD et al., 2010; DAI et al., 2018; JAUD et al., 2019). When coupled with others collected in the field, DEMs and orthophoto mosaics' spatial data provide value to analyzing geomorphic changes (BLANCHARD et al., 2010; JAUD et al., 2019, 2020). For example, detailed assessments of shoreline change rates generated through high-resolution imagery obtained with RPA add vital information for decision-making in coastal zone planning (NAGDEE et al., 2020). RPA data, when complemented with field collection of surface sediments for textural classification, makes the analysis more robust for decision-making in coastal management (PITMAN et al., 2019).

In Brazil, we highlight the work developed by Albuquerque et al. (2018a; 2018b) in the characterization of impacts and risk management results of extreme high-energy events on the extreme southern coast of Brazil. Silva et al. (2019) applied RPA-based geotechnologies to map eroded areas of the coastal zone on the southern coast of Rio Grande do Norte. Simões and Oliveira (2020) applied RPA data to study shoreline variation in the Mostardense resort between 2016 and 2017. Recently, Almeida et al. (2021) applied the RPA technology in characterizing the geomorphometry and morphological behavior of the coastal drainage channels in the Balneário de Cassino resort with a focus on DEM generation.

Morphological changes are always associated with sediments' removal and consequent transport from one point to another (SUGUIO, 2003). These changes may occur on the beach by exchanging accommodation space from one point to another on the same beach, from the beach to the inner continental shelf, and vice-versa, from

the beach to the dune deposit or in the opposite direction (SOUZA et al., 2005; SUGUIO, 2010; BARROS, 2018). These changes can be detrimental to tourism activity when they result in significant losses compared to gains (SOUZA et al., 2005).

Peroba and Redonda are tourist areas on the coast of the municipality of Icapuí, where erosive trends are currently detected on the coastline already described by Meireles and Santos (2012), Portela et al. (2014), and Costa (2019). This study is the first of those already developed in the municipality of Icapuí that combines data acquired with RPA and sediments collected in the field in coastal monitoring with the objective of (1) analyzing the volumetric variation by estimating the rate of change; (2) calculating shoreline mobility rates; and (3) analyzing the granulometric distribution of sediments as a function of their descriptive statistics.

2. Study Area

The Icapuí Municipality is located at the eastern end of the coastal area of Ceará State, Northeast Brazil (Figure 1). The study area consists of two beaches located west of the coast of Icapuí: Praia de Peroba (easternmost, here called Site 1) and Praia de Redonda (Site 2, westernmost) in an extension of about 5 km.

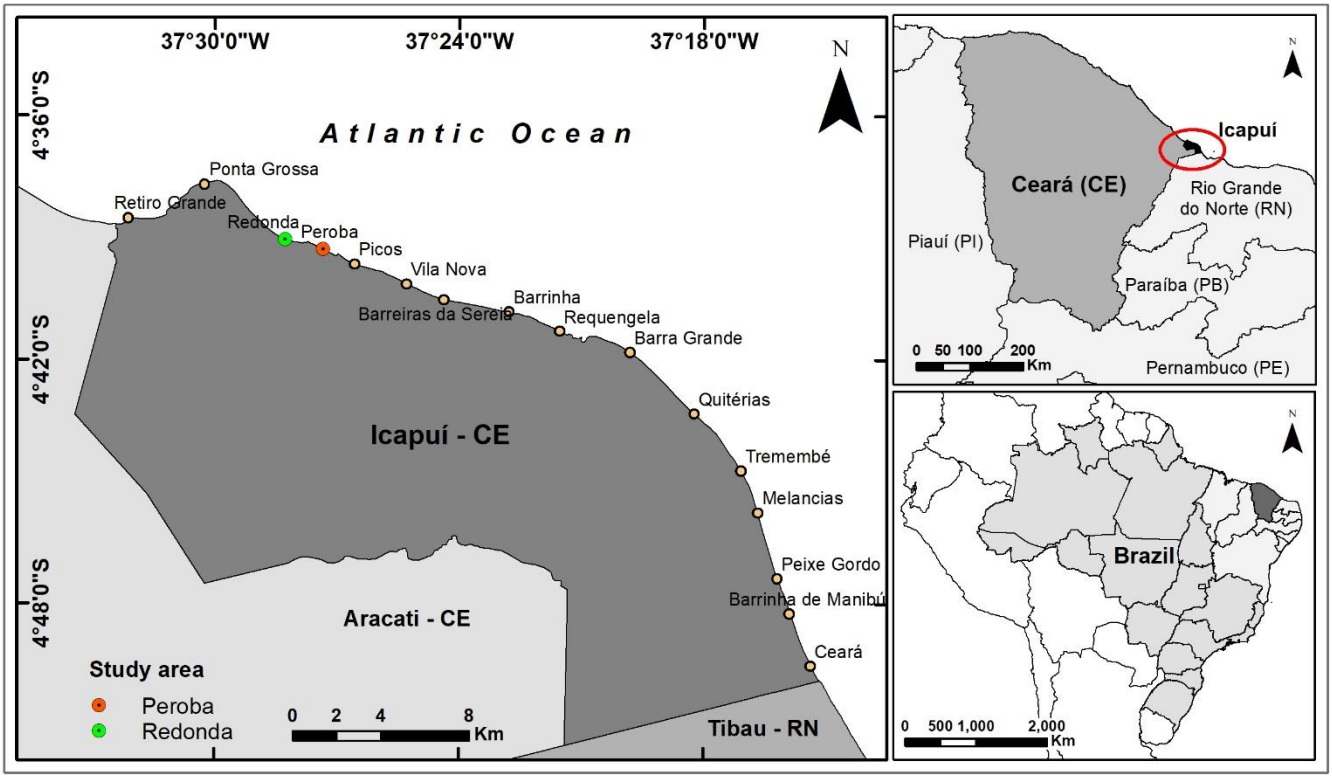

Figure 1. Location of the study area in the municipality of Icapuí - Ceará, Northeast Brazil.

The rainfall in Icapuí covers the months of February to May, with an average of 1,331.7 mm (MEIRELES; SANTOS, 2012). The average annual temperature is around 26° C (IPECE, 2007). The lowest temperatures occur during the rainy season (PINHEIRO et al., 2016). The predominant wind directions on the coast of Ceará are from SE, ESE, E, and NE, with average speeds that reach over 4.5 m/s in the drier months, reaching an average speed above 11 m/s, with the occurrence of SE winds in the dry season. In contrast, in the rainy season, the scenario reverses with the appearance of the Intertropical Convergence Zone (ITCZ), predominating NE winds (MEIRELES; SANTOS, 2012).

The waves that reach the coast of Icapuí are predominantly of the Sea type - about 80% - with periods between 1 and 9 seconds, and 20% of the Swell type with periods above 10 seconds (PINHEIRO et al., 2016). The significant wave height predominant in Aracati, the municipality closest to Icapuí on the east coast of Ceará, presents a frequency between 1.3 and 1.73 m (PINHEIRO et al., 2016). In the five field campaigns, measurements made in the surf zone showed values between 0.8 and 1.0 m with periods between 3.72 and 6.56 s.

3. Materials and Methods

3.1. Aerophotogrammetric data acquisition

Remotely Piloted Aircraft (RPA) enabled the imaging of the area studied. A Mavic 2 Pro model from the manufacturer DJI was used in this study. It is a multi-rotor aircraft weighing 900 g. It can safely operate up to 18 km from the radio transmitter and with a flight range of up to 31 min under optimal favorable weather conditions (see Table 1 and Figure 2A). When compared to satellite imagery, RPA data is free of noise, such as cloud cover. Using a Global Navigation Satellite System (GNSS) receiver in Real Time Kinematic (RTK) mode, control points distributed in the study area were acquired for georeferencing the products and assessing the accuracy of the method (Figure 2B).

Table 1. Specifications of the sensor used in the airborne data survey.

Camera Model	Resolution	Focal Distance	Pixel Size
L1D-20c (10.26 mm)	5472 x 3648	10.26 mm	2.41 x 2.41 um

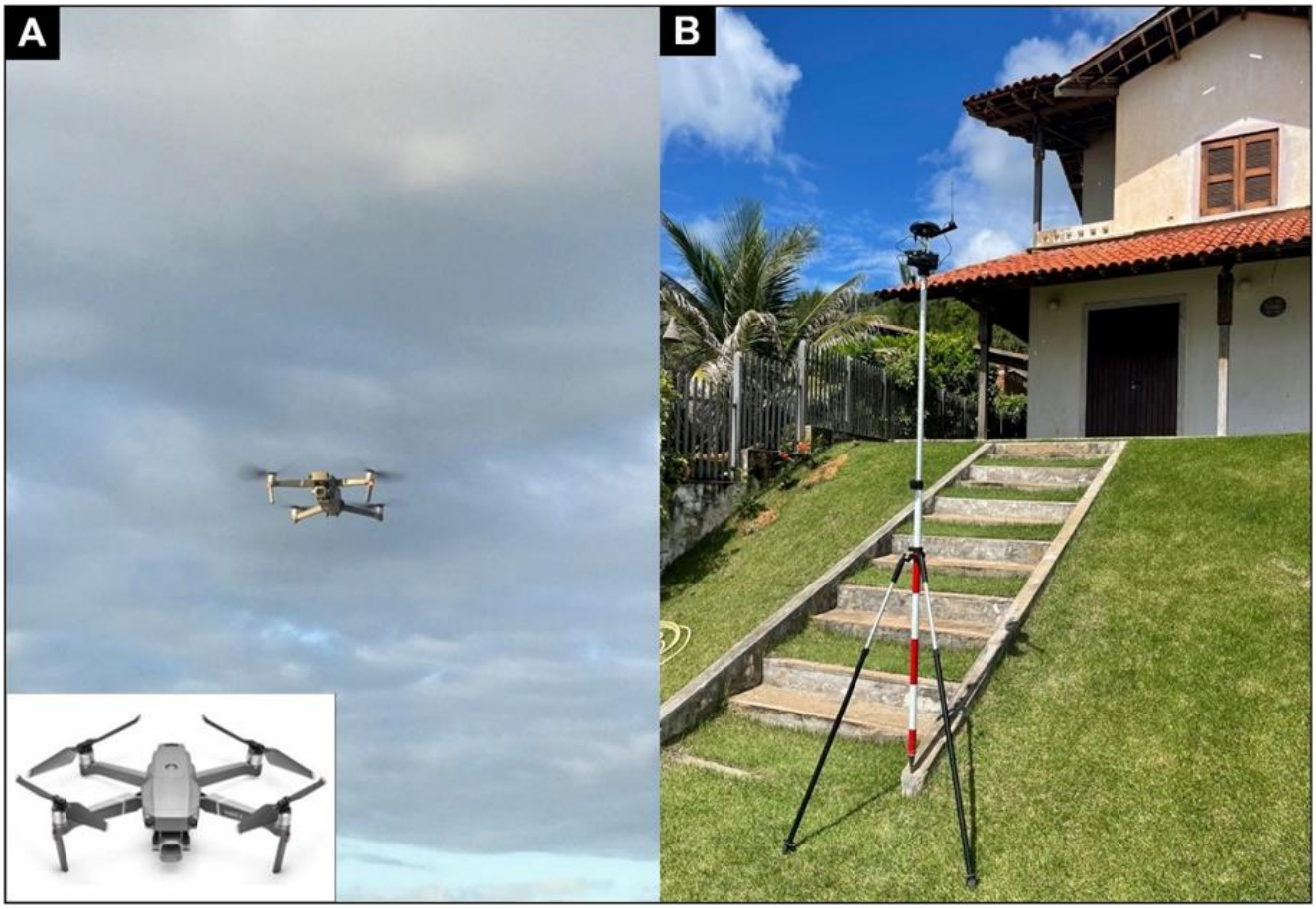

Figure 2. Field data collection. (A) Flight survey for aerophotogrammetric data collection with RPA; (B) Control point data collection with GNSS receivers.

Control points are essential to define the accuracy in positioning the images obtained in the field (ALBUQUERQUE et al., 2018a; PAGÁN et al., 2019). The points were processed based on the Brazilian Geodetic System (SGB) for subsequent photo-pointing of the images to reduce the Root Mean Square Error (RMSE) in the generation of aerophotogrammetric products, highlighting the Digital Surface Model and the Orthophoto mosaic. The points were used in the images georeferencing to maximize the survey's accuracy.

The flight planning process is a critical stage in the photogrammetric survey. It is the first stage of the work, usually involving integration between the demands of space, coverage, and photographic scale (BRASINGTON et

al., 2003). This process required a reconnaissance field of the study area, where the area's geomorphology contributed to the definition of the minimum height of the flights.

The flights were planned using the mobile application Map Pilot Pro from Drone Made Easy, where flight height, overflight area per sector, the overlap between images and tracks, camera incidence angle, and altitude were defined. The flight heights were set at 120 m, covering about 5 km of coastline. In aerial surveys, a frontal overlap of at least 75% and 60% is often recommended for lateral overlap (JANUŠAITĖ et al., 2019). Some authors apply the lateral overlap of 70% and 80% (JAYSON-QUASHIGAH et al., 2019; EICHMANNS; SCHÜTTRUMPF, 2021). This work applied the lateral and frontal overlap of 75%.

Five data collection camps were conducted over three months between August 2020 and August 2021 (see Table 2). The flights surveyed were designed to take the direction perpendicular to the coastline, covering mainly the surf zone, beach, and back beach, having extended to the residential area by the sea, as the control points were materialized in these portions. The piloting was in automatic mode, previously programmed before the field. The meteorological and oceanographic conditions (wind, precipitation, and tide) were considered before the flights. In this context, the wind needed to be favorable, without rain and a low tide of syzygy, for better coverage of the beach environment's features.

Table 2. Flight site, images, and flight dates.

Site 1		**Site 2**	
Images	Flight dates	Images	Flight dates
487	19th August 2020	782	20th August 2020
470	17th November 2020	797	18th November 2020
490	11th February 2021	772	12th February 2021
520	27th May 2021	802	28th May 2021
703	24th August 2021	1.005	23rd August 2021

3.2. Aerophotogrammetric data processing

The processing started with manually filtering all images collected in the field, where the non-vertical and blurred photos were removed to enable the construction of the orthophoto mosaic based only on nadir photos. Such photographs are those in which the angle between the horizon line and the camera lens is 90 degrees, with a tolerance of three degrees, more or less (SIMÕES; OLIVEIRA, 2020).

The selected images were inserted and processed in the Agisoft Metashape Pro software, based on SfM (Structure from Motion) algorithms and dense image correlation, with tools that facilitate the process of creating the DEM, orthophoto mosaic, and other associated products, allowing the construction of 3D coastal topography from a 2D image. (CHEN et al., 2018; DAI et al., 2018; JAUD et al., 2019; JAYSON-QUASHIGAH et al., 2019; PAGÁN, et al., 2019; PITMAN et al., 2019; SIMÕES; OLIVEIRA, 2020; EICHMANNS; SCHÜTTRUMPF, 2021). The advent of algorithms based on SfM innovated the area of three-dimensional topographic surveys, offering in an agile way the generation of 3D point clouds through acquisitions with affordable costs (SMITH et al., 2015).

To make the comparison between the produced mosaics possible and improve the data accuracy, these must go through two processes: registration and georeferencing (SIMÕES; OLIVEIRA, 2020). In this case, the photo-pointing process was performed. The data of materialized control points collected in the field from GNSS receivers were identified in the photographs (Figure 3). The georeferencing and processing were unique for both sectors, resulting in the Root Mean Square Error (RMSE) of the control and verification points being less than 3 and 2 cm, respectively.

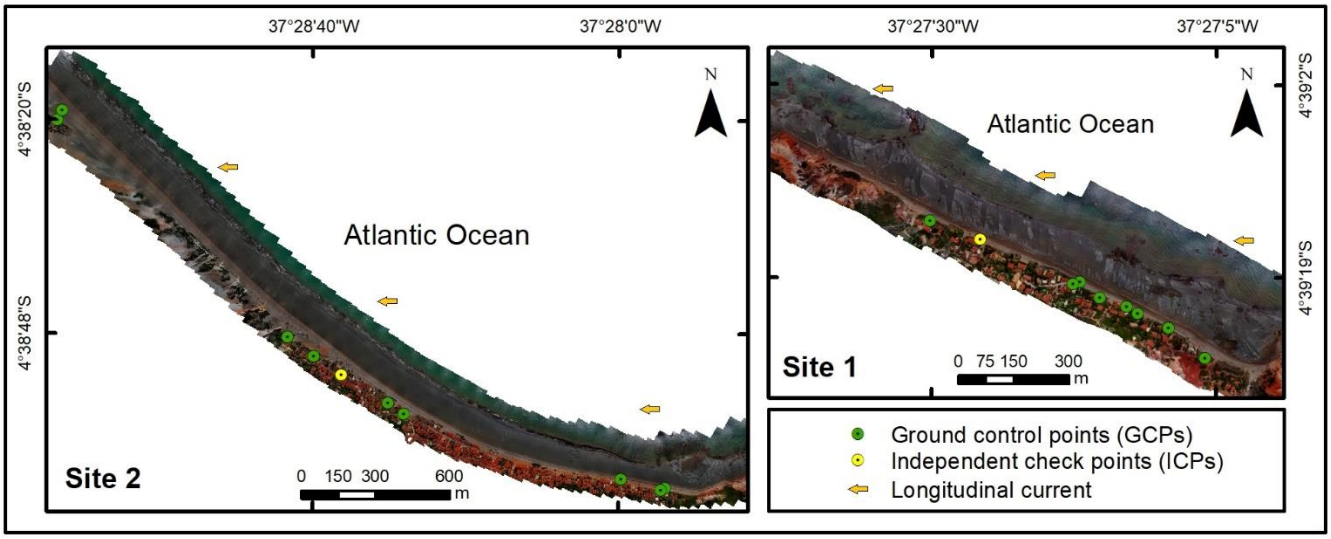

Figure 3. Spatial distribution of control points in the two sectors.

3.3. Geomorphic change analysis

The extracted DEMs were transferred to ArcMap, ESRI's ArcGIS software component. An area common to all the surveys was defined using a polygon to cut out the DEMs and subsequent application of the Difference of DEM (DoD) method using the Cut Fill tool. The generated DoDs spatialize the volume variation with better representativeness (JAUD et al., 2019). The method for assessing morphological variation by generating DoDs was based on the applications of Brasington et al. (2003), Wheaton et al. (2010), Jaud et al. (2019), and Jayson-Quashigah et al. (2019) and consists of the difference in elevations between the recent DEM by the previous one, as shown in Eq. (1):

$$\Delta DEM = Z_{post} - Z_{prev} \quad (1)$$

Where ΔDEM is the DoD, Z_{post} is the recent DEM and Z_{prev} is the previous DEM.

The total individual RMSE resulting from the image processing for the two sectors was used as the uncertainty for each DEM generated. The individual errors of the DEMs can be propagated to the DoD, constituting the total error (BRASINGTON et al., 2003; LANE et al., 2003; WHEATON et al., 2010; CHEN et al., 2018) and can be estimated based on Eq. (2).

$$\delta u = \sqrt{\delta z_{prev}^2 + \delta z_{post}^2} \quad (2)$$

Where δu is the error propagated to the DoD, δz_{prev}^2 is the error of the DEM of the preceding period, and δz_{post}^2 is the error of the DEM of the later period.

Morphological change volume and area estimation are extremely sensitive to the minimum detection limit (minLoD) (WHEATON et al., 2010). This propagated error has been used as a minimum detection limit (minLoD) level to distinguish fundamental surface changes from inherent noise (BRASINGTON et al., 2003; WHEATON et al., 2010; JAYSON-QUASHIGAH et al., 2019).

3.4. Annual shoreline change

The coastlines were manually vectorized based on the orthophotos obtained in the field between August 2020 and August 2021, considering the contrasting mark between the wet and dry strips in the syzygy tide, the base of active cliffs, erosive scarps and bases of coastal protection structures following the method already applied by Del Río et al. (2012) and Jayson-Quashigah et al. (2013).

The Digital Shoreline Analysis System (DSAS) was applied to analyze the changes in the shoreline. To obtain the best detailing of the changes that occurred in the analyzed period, a distance of 10 m between the generated transects was defined (JAYSON-QUASHIGAH et al., 2013; SILVA NETO et al., 2020; CHACANZA et al., 2022). The rate of shoreline change was obtained by applying the linear regression statistic (LRR) using the following

classes according to Chacanza et al. (2022): severe erosion (less than -3 m/year); moderate erosion (between -3 and -2 m/year); low erosion (between -2 and -1 m/year); stability (-1 and +1 m/year); low deposition (between +1 and +2 m/year); moderate deposition (between +2 and +3 m/year); and severe deposition (greater than +3 m/year). This parameter considers all the lines that the transects cross, allowing the launched transects to be analyzed individually (HIMMELSTOSS et al., 2018). The RMSEs of shoreline positioning were estimated based on the individual errors of each image processing, which can be calculated using Eq. (3) (JAYSON-QUASHIGAH et al., 2013).

$$E = \left(\sqrt{E_1^2 + E_2^2 + E_3^2 + \cdots + E_n^2}\right) * T^{-1} \quad (3)$$

where E_1, E_2, E_3, ..., E_n correspond to the individual shoreline position errors, and T is the time interval under analysis (AIELLO et al., 2013; JAYSON-QUASHIGAH et al., 2013).

3.5. Sediment grain size analysis

A total of 102 surface sediment samples were collected in five field campaigns over 12 months. The samples were distributed in the back beach, backshore, and nearshore zones of nine monitoring points at Peroba and Redonda beaches. In the field, samples were collected using a spatula at 10 to 15 cm depth. After collection, the samples were taken to the Laboratory of Marine and Applied Geology (LGMA) at the Geology Department of the Federal University of Ceará. In the granulometric analysis, the sieves of 2.0, 1.0, 0.5, 0.25, 0.125, and 0.062 mm were used, according to the textural limits established by Wentworth (1922). The results of granulometry were inserted in the ANASED sediment analysis software available at the LGMA, where the statistical parameters were calculated based on the traditional distribution model of Folk and Ward (1957), namely average diameter, asymmetry, and standard deviation (degree of selection).

4. Results

Five DEMs were generated, with spatial resolutions of less than 24 cm. The orthophotos presented resolutions lower than 3 cm. The high resolution allowed better visualization of the details of the generated products, becoming a preponderant role in volume calculation and shoreline change analysis.

4.1. Morphological changes in Site 1 (Peroba Beach)

4.1.1. Sediment volume changes

Peroba Beach is about 1,570 m long, and the analyzed area was about 96,466 m². The altimetric variations in one year indicate altimetry between -4.7 and 3.8 m (Figure 4). The site is characterized by the absence of a recreational beach at high tide periods due to the total occupation of the Back beach zone.

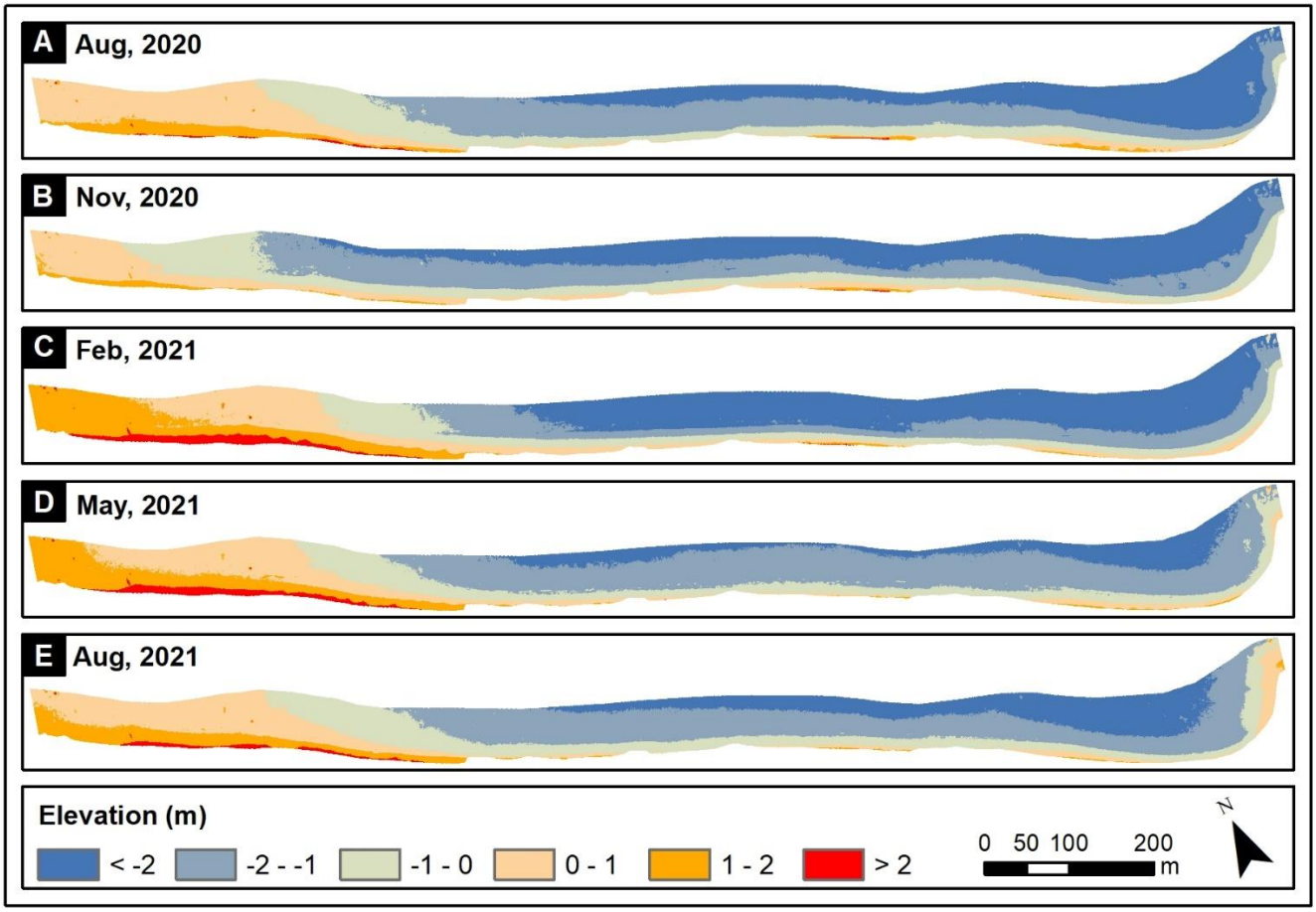

Figure 4. Individual DEMs from five periods were cut from data collected at Peroba Beach.

The results of the volume variation for Peroba Beach indicated a positive balance of 32% of sediments gained throughout the period analyzed between August 2020 and August 2021, on the order of 18,815 m^3 at a monthly rate estimated at 1,568 m^3/month. In this period, the volume of sediment deposited was calculated at about 24,059 m^3 and eroded at -5,244 m^3. The sediment input and output imbalance was approximately 32%, and about 75% of the beach experienced deposition (Figures 5E and 6). Between August and November 2020, the beach experienced an erosive process with sediment loss calculated at -27,061 m^3 (Figures 5A and 6). The periods between November 2020 and February 2021 and February and May 2021 registered successive depositions of sediments estimated at 32,235 and 22,042 m^3, respectively (Figure 5B, C, and 6). In the last period, between May and August 2021, the balance was negative in the order of -8,620 m^3 (Figures 5D and 6).

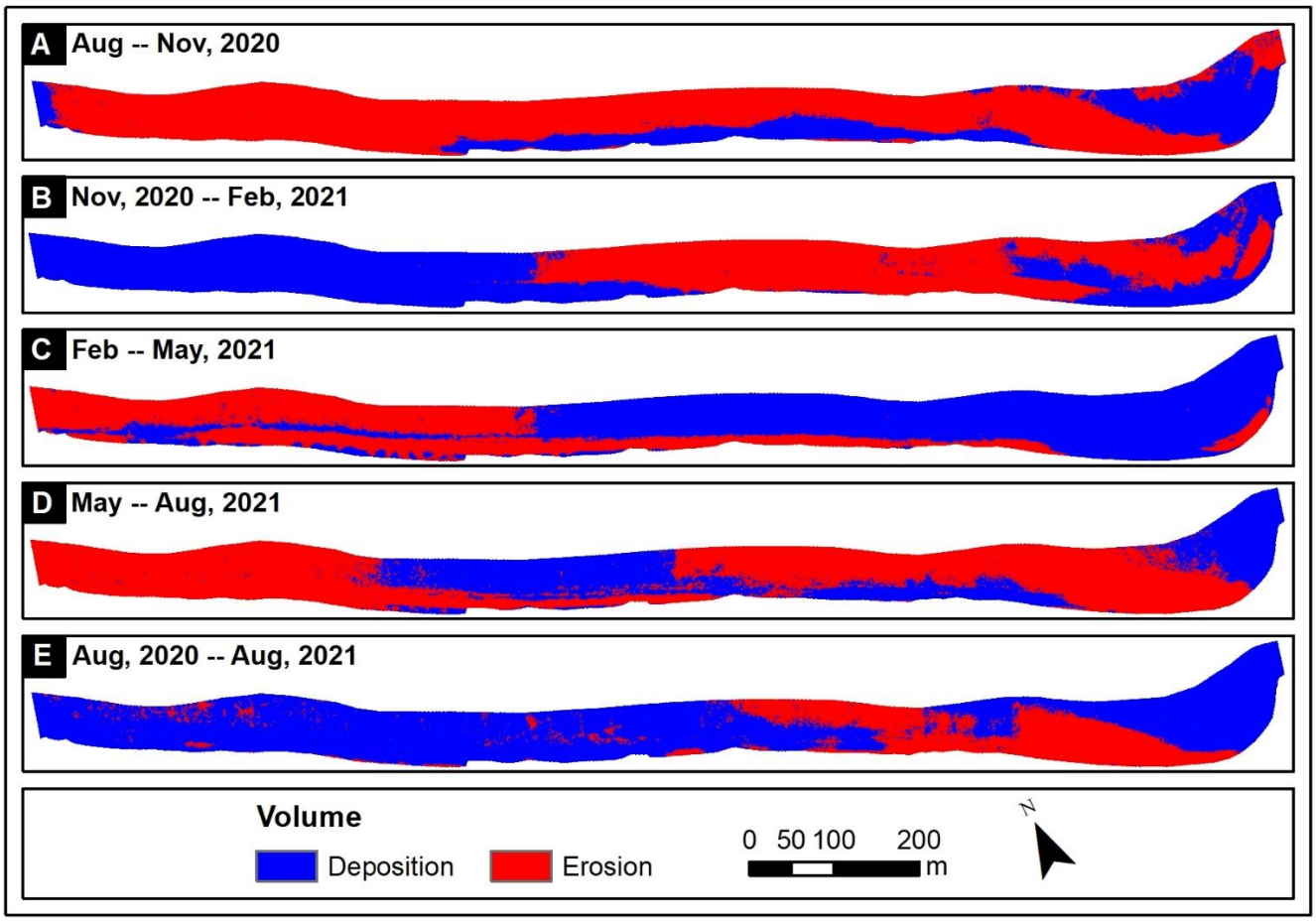

Figure 5. Spatial representation of variation in the volume of sediment eroded and deposited on Peroba beach.

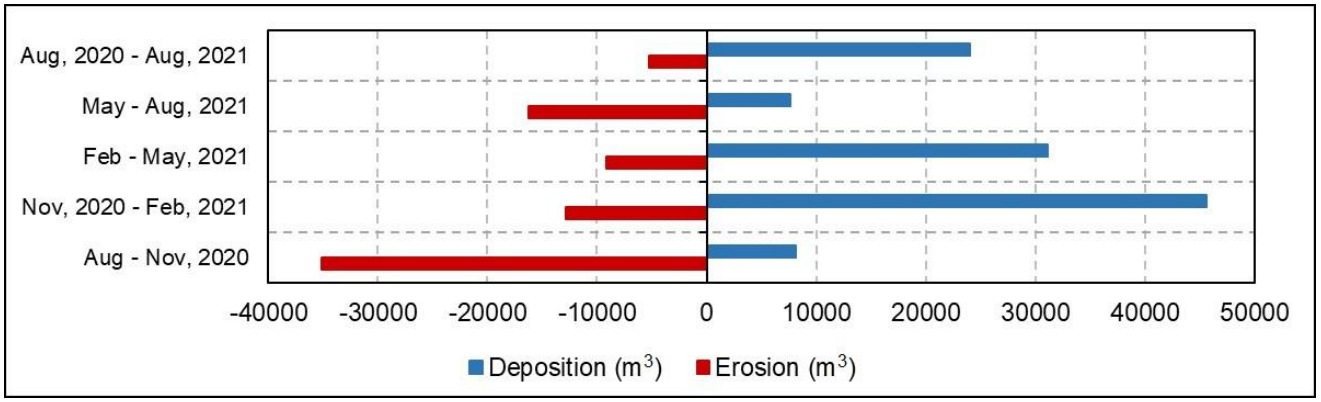

Figure 6. Sediment volume changes on Peroba Beach.

The variations in volume that occurred at Peroba Beach are also reflected in the series of topographic profiles generated from the DEMs (Figure 7). The variations that occurred at the eastern end of Peroba Beach indicated that the sediments eroded near the shoreline might have been remobilized and deposited toward the sea (Figure 7A). Losses above one meter occurred close to the shoreline in the central stretch of the beach (Figure 7B). In contrast, in the western end, more intense deposition occurred in areas close to the shoreline (Figure 7C).

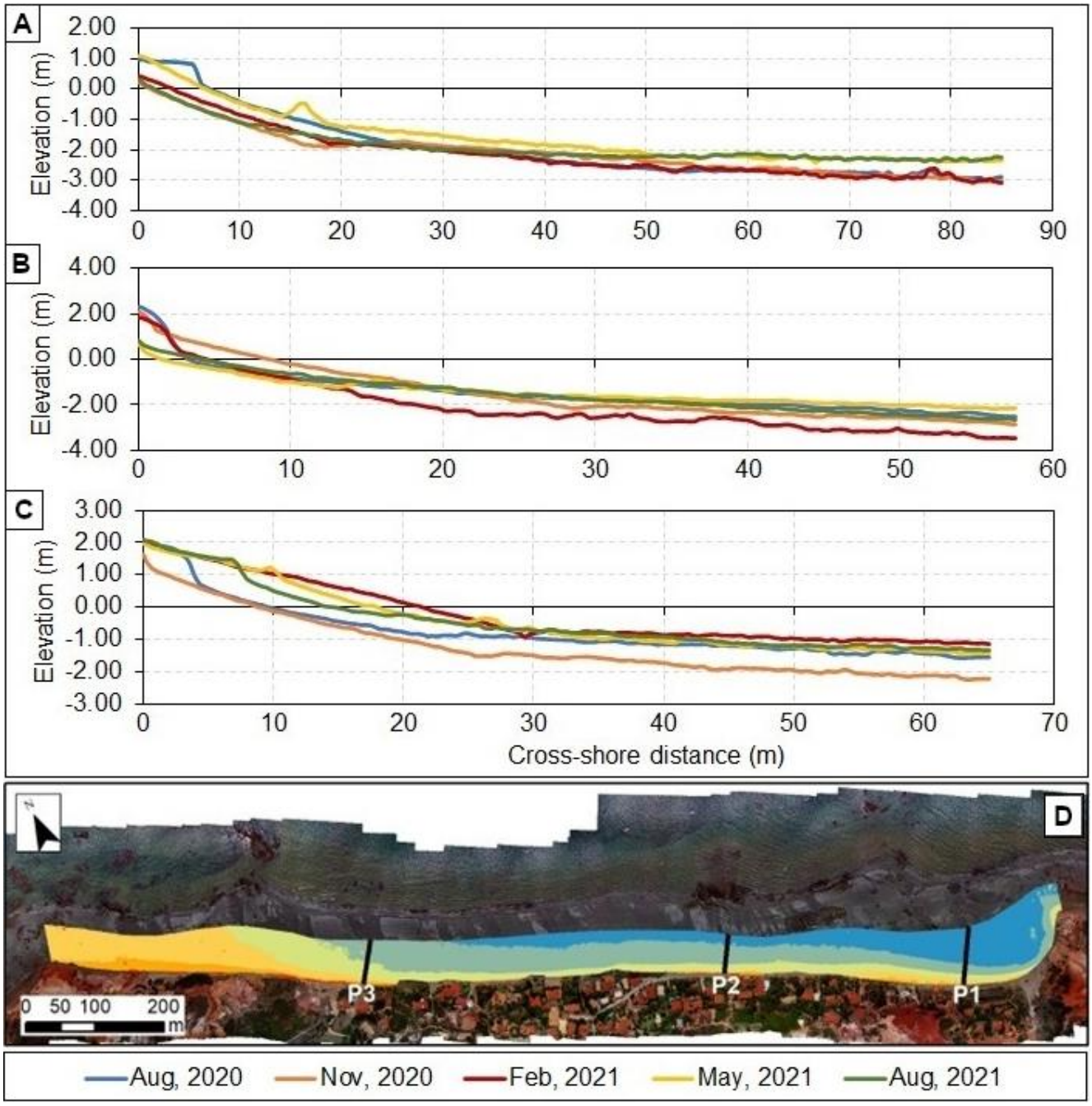

Figure 7. Cross-shore profiles show altimetric variations along Peroba Beach between August 2020 and August 2021. (A) Profile P1; (B) Profile P2; (C) Profile P3; and (D) Location of the profiles.

4.1.2. Variation of the shoreline between August/2020 and August/2021

Table 3 shows that between August 2020 and August 2021, the short-term shoreline change rate at Peroba Beach was estimated to be 0.87 m/year.

Table 3. Rates of change and linear shoreline motion for site one between August 2020 and August 2021.

Parameter	Min	Mean	Max	Standard deviation
LRR (m/yr)	-2.74	0.87	6.72	±2.28
NSM (m)	-6.01	0.32	6.18	±2.59

The average rate of change established from the linear regression statistics pointed to stability in the coastline. The apparent stability corroborates the stability that Silva Neto et al. (2020) identified when they analyzed the

shoreline mobility by applying satellite images at intervals above 10 years on the Icapuí coast. Figure 8 shows that the highest rates of shoreline retrogradation were recorded in the eastern stretch of the beach, and the highest rates of progradation in the western stretch.

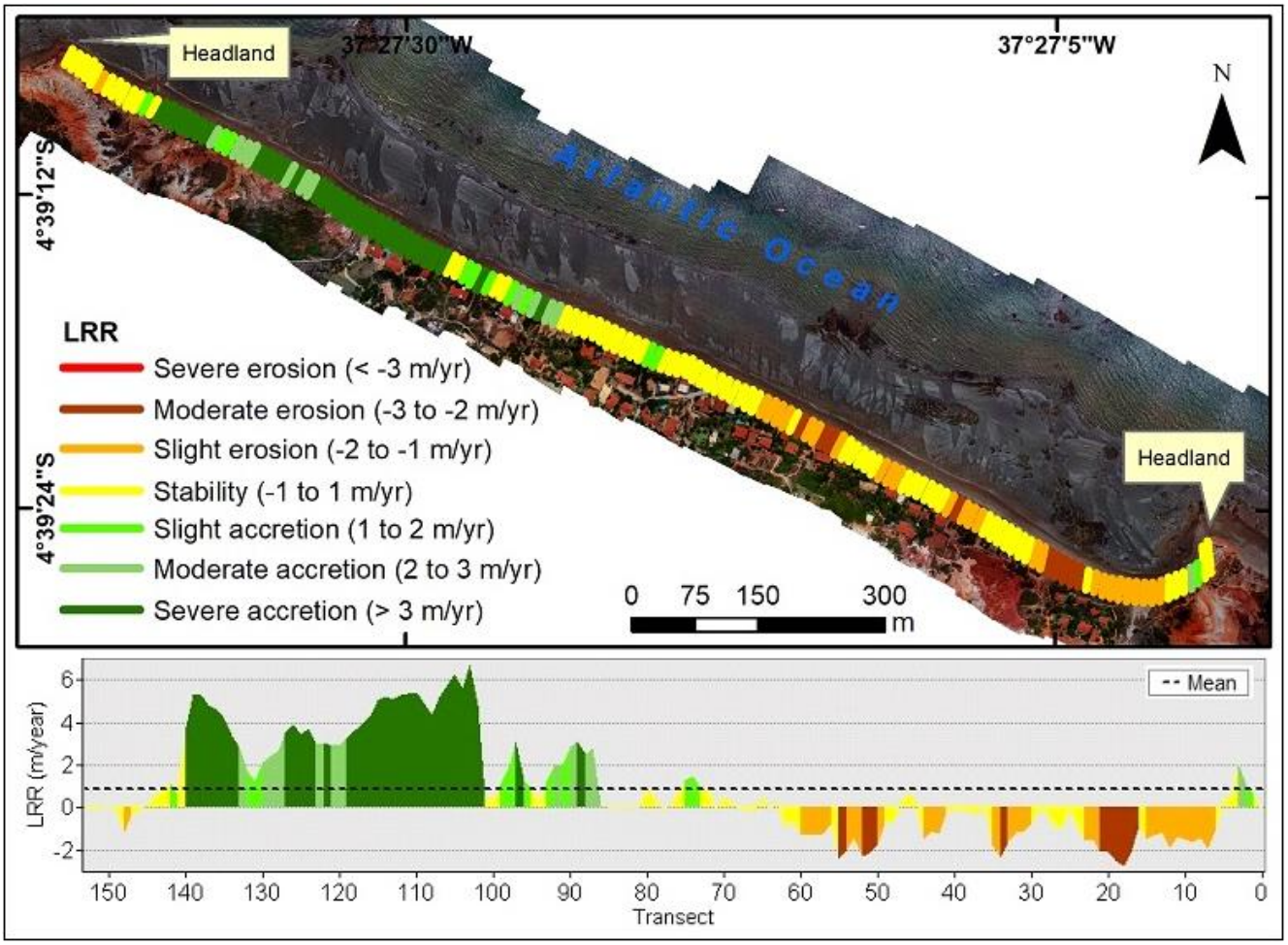

Figure 8. Spatial visualization and shoreline variation rate applied to the LRR parameter at Peroba Beach between August/2020 and August/2021.

4.1.3. Relationship between beach volume and shoreline dynamics at Peroba Beach

In this sector, the results of volume variation indicated trends similar to the shoreline (Figures 5E and 8). In all the analyzed periods, the sedimentary balance of volume variation and the shoreline variation rate were positive, with values of 18,815 m^3 and 0.87 m/year, respectively. Although the average variation of the shoreline presents a value that fits in the stability class, sediment loss in the beach's eastern end resulted in the shoreline retreat of up to 6 m (Table 3).

Erosion events on the eastern stretch of Peroba Beach threaten the destruction of houses (Figure 9B, C, E, and F). This has driven direct human interventions in constructing wood-based erosion containment structures on localized stretches of the beach (Figure 9B-F). These actions contribute to the temporary stabilization of the shoreline. On the other hand, deposition has occurred in the western stretch, resulting in the shoreline worsening up to 6 m (Table 3). These depositions remind us of a cyclical scenario of periods preceded by erosion and subsequent depositions in the area, as identified by Costa (2019). In a recent analysis of line variation on the stretch between Peroba and Redonda, Chacanza et al. (2022) also identified cyclical variations every five years of analysis over a 15-year interval. According to Silva and Oliveira et al. (2022), these cyclical events may be behind the division of opinions regarding the construction of coastal protection work, with a part of the local community being opposed and the other being favorable. According to Jayson-Quashigah et al. (2019), these two realities suggest adopting a sustainable management approach to the beach system to increase its resilience and users.

Figure 9. Mosaic of images representing erosional and depositional stretches. (A) Eastern view of Peroba beach; (B and C) Different views of the same eroded stretch with wooden coastal protection structures and repositioning of the access that had been destroyed; (D and E) Same stretch of beach where the first image of August 2020 presents a higher quota and the second of August 2021 with a lower account, a sign of sediment loss; (F) Erosive scarp, controlled by the community with constant reposition of sediments in order to maintain the access to the other infrastructures that are east of the beach; and (G-I) Images of three periods, at the survey point of profile P3, the first in August 2020 (G), second in November 2020 (H) and the third in August 2021 (I).

4.2. Morphological changes in Site 2 (Redonda Beach)

4.2.1. Sediment volume changes

Two distinct features represent site 2. The eastern stretch lacks a recreational beach in periods of high tide, with the back beach completely occupied by residences and inns. On the other hand, the western stretch is practically unoccupied because it is a preserved area integrating the environmental reserve that extends until the Ponta Grossa beach, located further west of the area. In this sector, the analyzed area was about 214,321 m². The altimetric variations during the analyzed period indicated altimetry between -4.7 and 8.2 m (Figure 10).

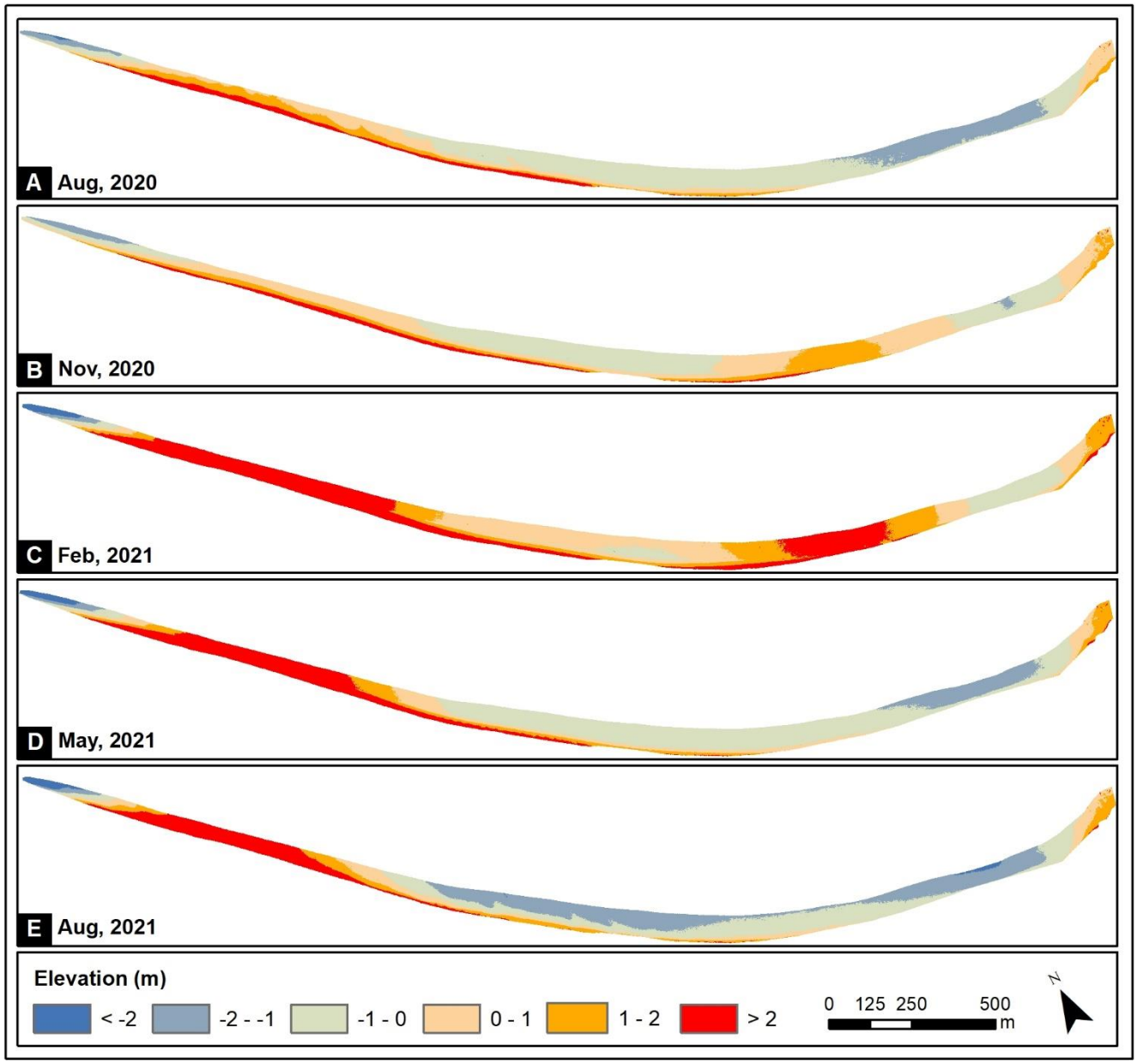

Figure 10. Individual DEMs from five periods were cut from data collected at Redonda Beach.

During the period analyzed, Redonda Beach had a negative sediment balance estimated at -1,230 m³, equivalent to a monthly rate of about -103 m³/month. About 72,719 m³ were deposited, and about -73,950 m³ eroded (Figure 11E and Figure 12). The imbalance between deposition and erosion was 0.4%. This value indicates that the sediment eroded at Redonda Beach was proportional to the sediment deposited in one year. The first two periods between August and November 2020 and November 2020 and February 2021 were marked by successive

deposition, with sediment gain estimated at 73,023 and 247,638 m^3, respectively (Figures 11A, B, and 12). Inverse processes occurred in the last two periods between February and May 2021. Between May and August 2021, sediment losses were estimated at -238,054 and -83,424 m^3, respectively (Figures 11C, D, and 12).

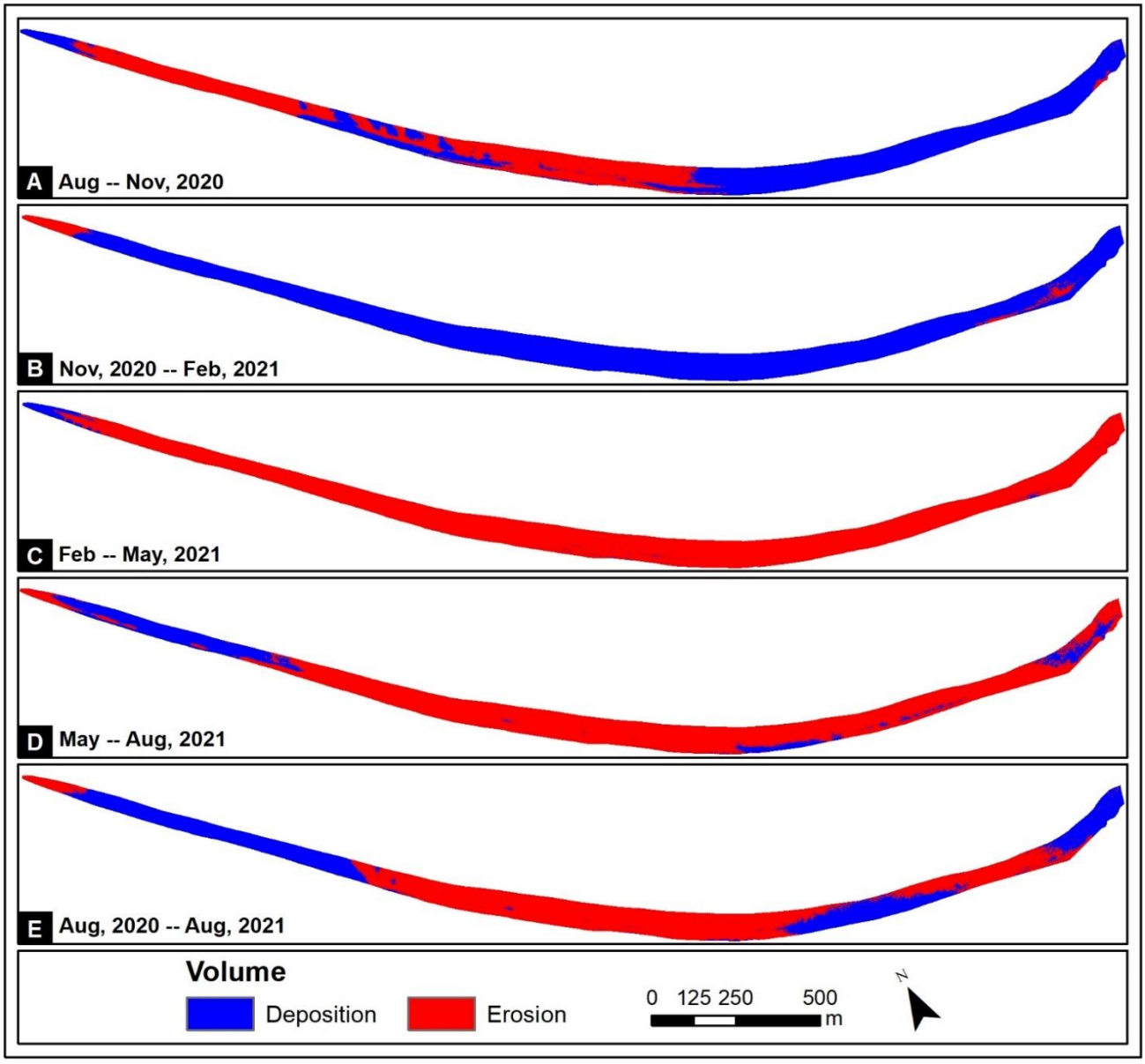

Figure 11. Spatial representation of variation in the volume of sediment eroded and deposited on Redonda Beach.

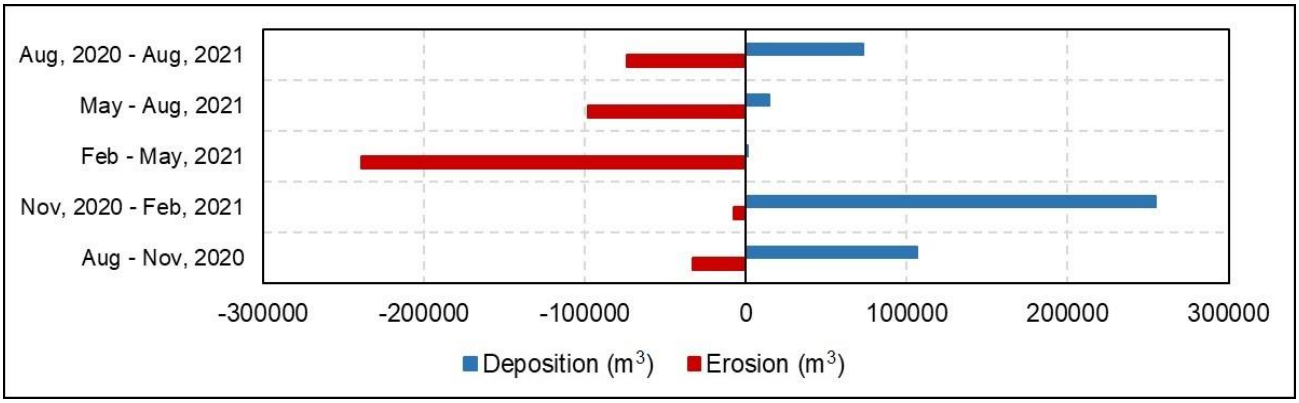

Figure 12. Sediment volume changes on Redonda Beach.

Sediment deposition in the western portion of the beach was also reflected in the topographic profiles, where variations exceeding one meter occurred between August 2020 and August 2021, resulting in the movement of the shoreline toward the sea (Figure 13C). In the same period, the erosion that occurred in the eastern and central sections of the beach also resulted in variations greater than one meter (Figure 13A, B).

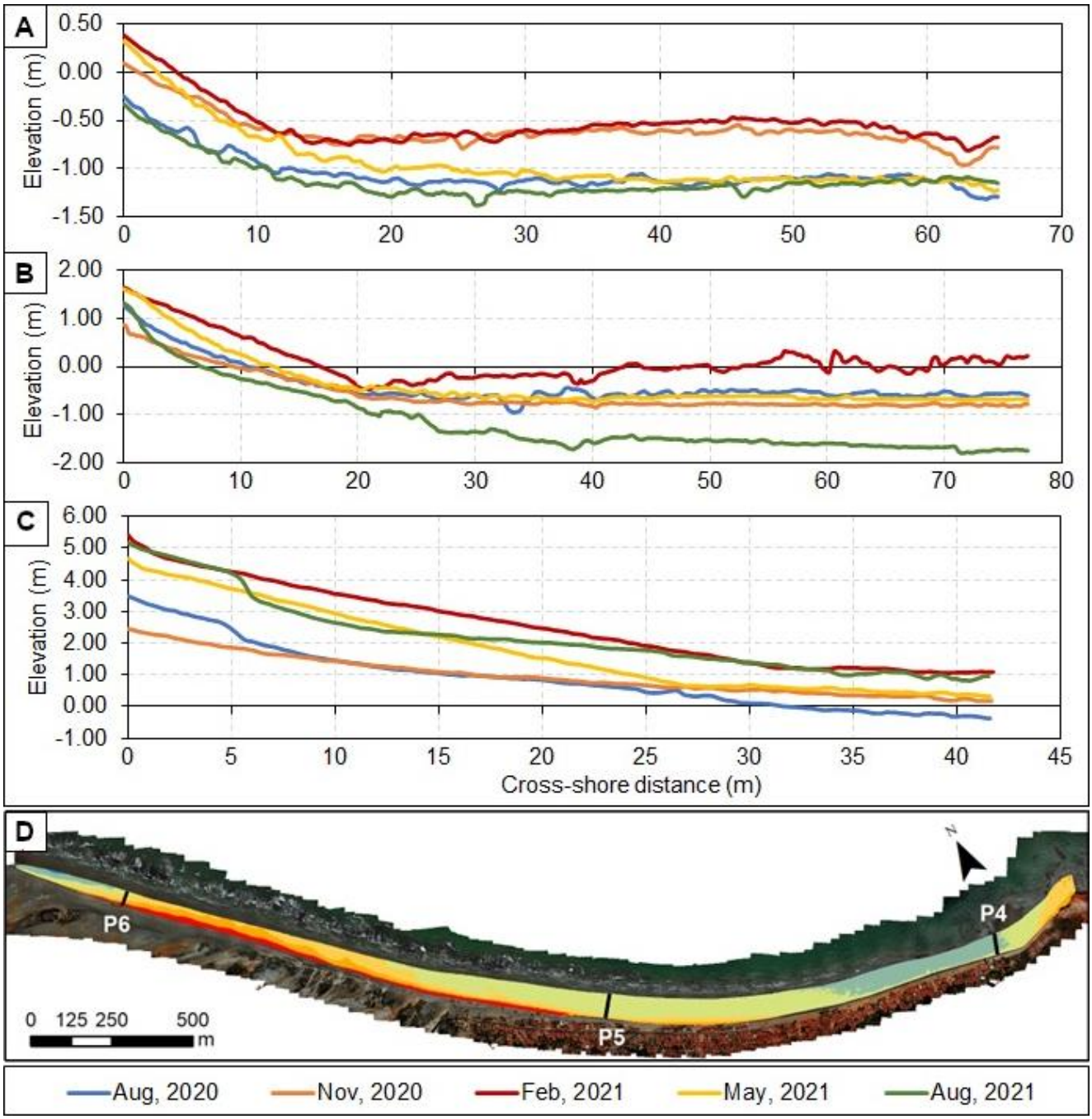

Figure 13. Cross-shore profile showing altimetric variations along Redonda Beach between August 2020 and August 2021. (A) Profile P4; (B) Profile P5; (C) Profile P6; and (D) Location of the profiles.

4.2.2. Variation of the shoreline between August/2020 and August/2021

Table 4 indicates that between August 2020 and August 2021, the short-term shoreline change rate in sector 2 was estimated at 1.27 m/year, the most significant retraction was estimated at -2.89 m/year, the largest attraction at about 6.04 m/year. In the eastern subsector of the beach was where the record of stability in the shoreline occurred, and in the western subsector occurred the highest progradation rates (Figure 14). In 12 months of monitoring, it was observed that the shoreline moved about 1.06 m towards the sea; the most significant

movements towards the sea were recorded in the western sub-sector with values that reached about 5.65 m. In the eastern sub-sector, minor variations were recorded, with the shoreline remaining stable in most of the beach stretch and small localized stretches where the retreat reached values close to 3 m (Table 4).

Table 4. Rates of change and linear shoreline motion for site two between August 2020 and August 2021.

Parameter	Min	Mean	Max	Standard deviation
LRR (m/yr)	-2.89	1.27	6.04	±1.76
NSM (m)	-2.97	1.06	5.65	±1.61

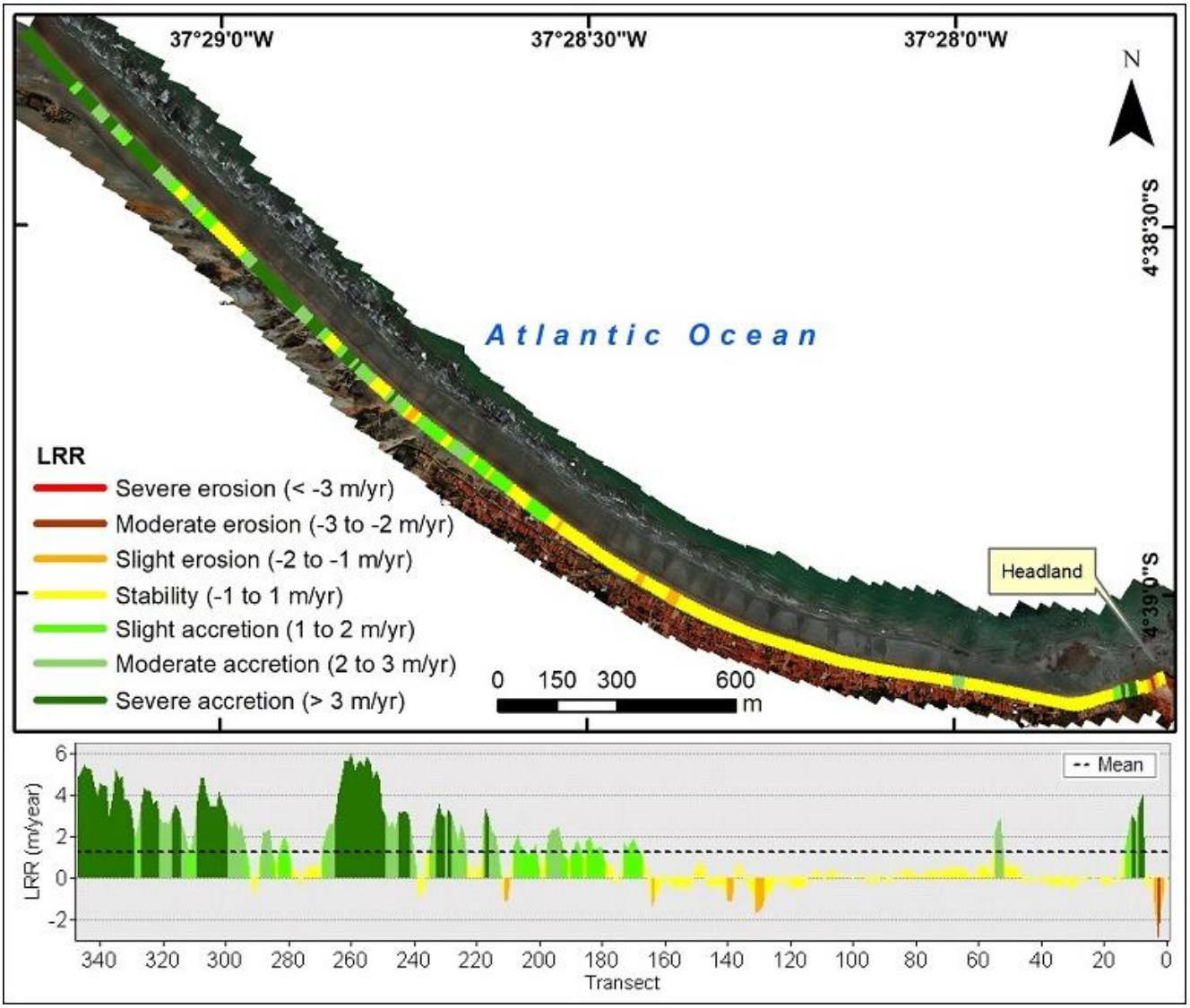

Figure 14. Spatial visualization and shoreline variation rate applied to the LRR parameter at Redonda Beach between August 2020 and August 2021.

4.2.3. Relationship between beach volume and shoreline dynamics at Redonda Beach

Results of volume variation pointed to a negative balance for Redonda Beach at about -1,230 m^3, where 61% of the beach underwent erosive processes. Despite the negative volume balance, in one year, the shoreline degraded by about one meter (Table 4). In this beach, the highest degradation rates occurred in the western stretch, with the line reaching advances higher than 5 m, which caused an increase in the width of the back beach and consequent reduction of the backshore. The wave attack associated with the smaller beach width may be at the origin of the erosive scarp appearance between May and August 2021 (Figure 15D). Human actions such as beach access may negatively impact the beach escarpment, where, by wind action, sediments may be eroded and

remobilized to form frontal dunes. The sediment volume losses in the beach's eastern and central sections did not influence the shoreline due to its fixation by a rigid coastal protection structure (Figure 15).

Figure 15. Mosaic of images: (A) West view of Redonda beach, showing a rock-fill coastal protection structure, which fixes the coastline; (B) Conclusion phase of the coastal protection work; (C) Incidence of waves on the protection structure; and (D) An erosive scarp more than half a meter high.

4.3. Sedimentary characterization

Analysis of 102 sediment samples collected during five field campaigns at 21 monitoring points distributed in the study area indicated, according to Shepard (1954) classification, that 87% of the samples were sandy and 13% were muddy sand. All samples classified as muddy sand were collected in the nearshore zone, mainly in the second half of the analyzed period. About average size, the sediments were composed of very fine sand at 49%, fine sand at 33%, medium sand at 17%, and coarse mud at 1%. Regarding asymmetry, 37% of the samples were classified with very negative asymmetry, 13% with negative asymmetry, 20% as approximately symmetric, 24% as positive asymmetry, and 6% with very positive asymmetry. The higher percentage of fine sediments reveals that the beaches may receive sediments from other sources.

Regarding the degree of selection, nearshore and back beach sediments were mostly moderately selected. Backshore samples were poor to moderately selected and fell between the very fine to medium sand ranges of

negative to approximately symmetric asymmetry. Back beach samples were moderately selected with medium sand classification ranging from positive to approximately symmetric asymmetry (Figure 16A).

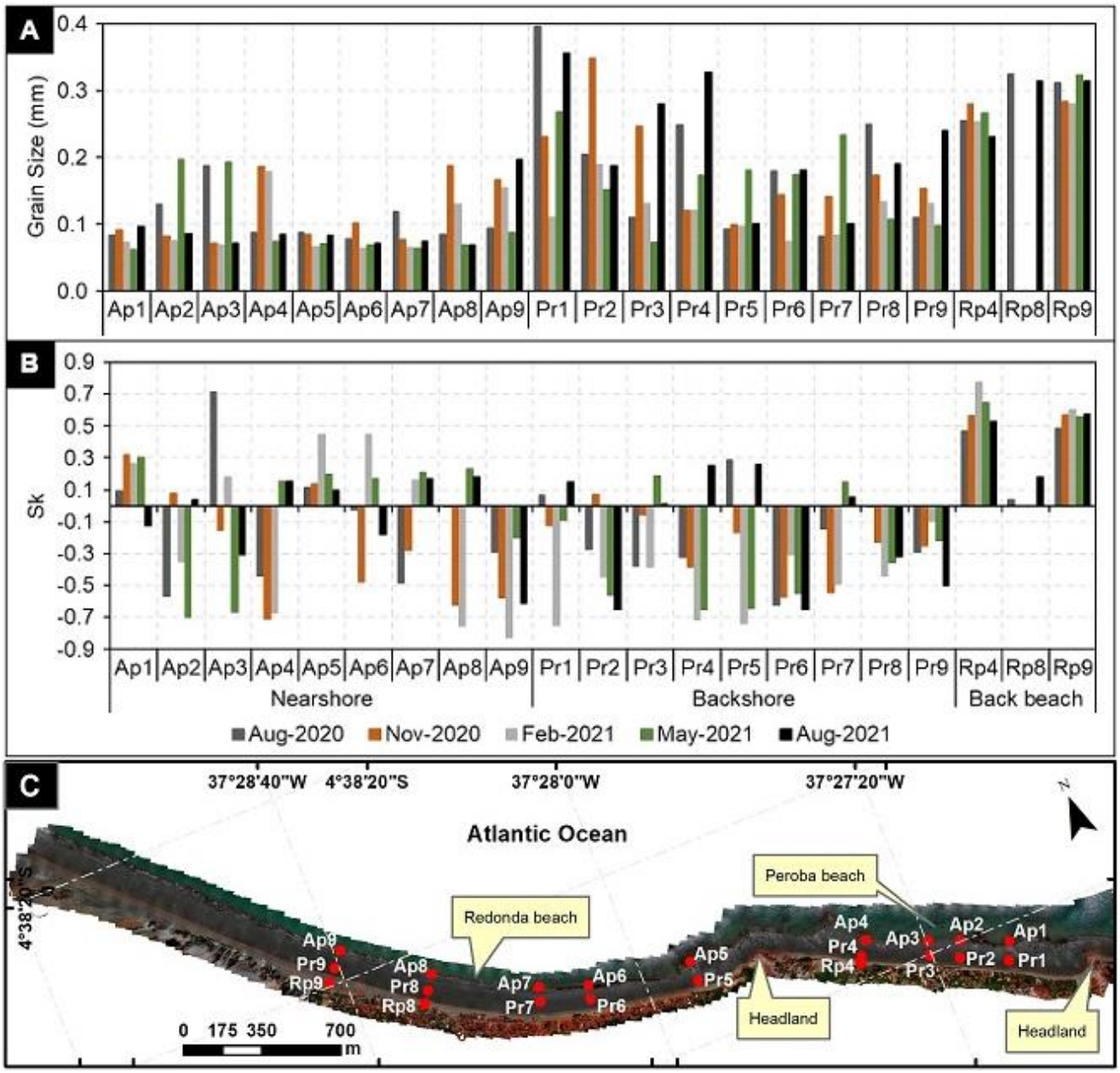

Figure 16. Sediments are distributed on the nearshore (Ap1 to Ap9), backshore (Pr1 to Pr9), and back beach (Rp4, Rp8, and Rp9) at nine monitoring points along the study area's coastline. (A) Mean grain size variation; (B) Sk asymmetry; and (C) Sediment sample locations.

In beaches, sands that generally present classifications from moderately to well-selected indicate that the sediments come from a source with the same characteristics (MARTINS, 2003; BARROS, 2018). Finer sediments are generally well-selected (MCLAREN; BOWLES, 1985). In this case, they were mostly of moderate selection. On-site, poorly sorted grades may be associated with eroded sediments from active cliffs and by direct interaction of the beach with the frontal dune system through the sediment transfer bypass effect. In coastal processes, whenever the sediment size becomes finer, the asymmetry tends to be more negative, with fine and light grades tend to be eroded and transported more quickly than heavy ones (MCLAREN; BOWLES, 1985), reflected in Fig. 16B. Negative asymmetry arises when fine sediments are removed by the backwash separation process, giving way to coarser sediments due to the high wave energy that the beach is subjected to where the addition of coarser material can

also cause it. Positive asymmetry is the competence of the transport agent in the one-dimensional flow (MARTINS, 2003).

The concentration of sediments of very fine sand fraction and negative asymmetry located in the eastern portion, immediately to the downdrift of the promontory at Redonda Beach, may be associated with the combination of rocky outcrops existing at the site that act as an abrasion platform, directly influencing the wave and tide currents that reach the beach, consequently changing the granulometric parameters, by the incompetence of the transport agents. The transport and deposition process of the finest asymmetrically negative superficial sediments generally occurs when the energy decreases and the coarsest and most asymmetrically positive when the energy is high (MCLAREN; BOWLES, 1985).

Sediments of finer fractions have less space between particles, which reduces water percolation, and sediment transport may occur with intensity during wave ebb than in spreading (NORDSTROM, 2010). They are quickly suspended, removed from the beach, and deposited into the sea (NORDSTROM, 2010; JAYSON-QUASHIGAH et al., 2019). The percolation rate increases as the sediment fraction increases (PITMAN et al., 2019). These conditions may be associated with deposition in the western portion, especially Redonda Beach.

Sediment erosion, transport, and deposition vary over different time scales and may be influenced by tidal seasonality, longitudinal current, wave energy, and changing seasons throughout the year (QI et al., 2022). On the other hand, the presence of very fine sediments in the easternmost portion of Redonda Beach indicates that the littoral drift is not the essential contributing factor in mobilizing fine sediments to the site.

5. Discussion

It was observed that the stretches of relatively stable coastline have anthropic influence by constructing erosion containment structures. The higher rates of sediment degradation and deposition that occurred in the west stretch of Peroba Beach as well as in Redonda Beach may be related to the erosion of the eastern areas of the two beaches because the positive sediment balance in Peroba Beach and negative in Redonda beach, indicate that there must be other sources of input feeding the beaches through coastal drift. Although the average variation rates of the coastline were positive on both beaches, the presence of rigid coastal protection works in Redonda Beach and the constant local interventions in localized stretches of Peroba Beach indicate coastal erosion. Generally, the interventions condition the hydrodynamic action modifying the sediment transport system and may accelerate or retard erosive or depositional processes (COWELL; THOM, 1994). If the coastal interventions are by longitudinal works often limit the evolution of the coastline (SOUZA et al., 2005; COSTA; COELHO, 2013; BORETTO et al., 2018; GRIGGS; PATSCH, 2019), existing characteristics in Redonda Beach.

Barros (2018) mentions that in Icapuí, events such as super high tides, ebb tides, and ocean swells associated with the low topographic gradient of the beaches are significant causes of coastal erosion where during the tidal transgression process, sediments are eroded from the berm and are directed out to sea. The reverse process happens during the regression, with deposition occurring on the berms.

The erosion prevalent at the eastern ends, especially immediately southeast of the promontories on both Peroba Beach and Redonda Beach, may be associated with the refraction effect of the waves when they hit the promontories. The eroded sediments are transferred to the entrances, those deposited at updrift are retained, allowing the area to fatten up, and those deposited at downdrift are transported by the action of littoral drift and deposited in the western portions, which is particularly important given the curvilinear shape of Redonda beach. Portela et al. (2014) reported erosion events on Redonda Beach due to wave attacks. Recent studies on Peroba and Redonda beaches analyzing shoreline variation between 2005 and 2020 highlighted erosion trends over 15 years and cyclical changes in short-period analysis (CHACANZA et al., 2022).

Coastal processes that result in changes in shoreline position are also highly influenced by climate change, on a global scale with sea level rise and on a local scale by the change in wave climate, making the coasts vulnerable to the occurrence of flooding or coastal erosion (MASSELINK et al., 2016). Wave data from the Wavewatch III global model indicated that as it approaches August, there is a trend in the increase of significant wave height with periods ranging between 5 and 8 seconds (Figure 17). In this period, the wind speed has also been high. Between 2020 and 2021, despite being a period dominated by the passage of the La Niña phenomenon, which often coincides with abundant rainfall. Rainfall in the municipality of Icapuí was low during the period under analysis, and this scarcity of rain in areas like Icapuí, where there is no major watercourse, means that erosion processes tend to be

progressive. The erosion in the far east and fattening of the western stretches of the Peroba and Redonda beaches may be related to what Muehe (2011) states that low rainfall and strong winds in the Northeast Region favor the formation and fattening of dune fields resulting in negative sediment budget on the beaches and the consequent variation of the shoreline.

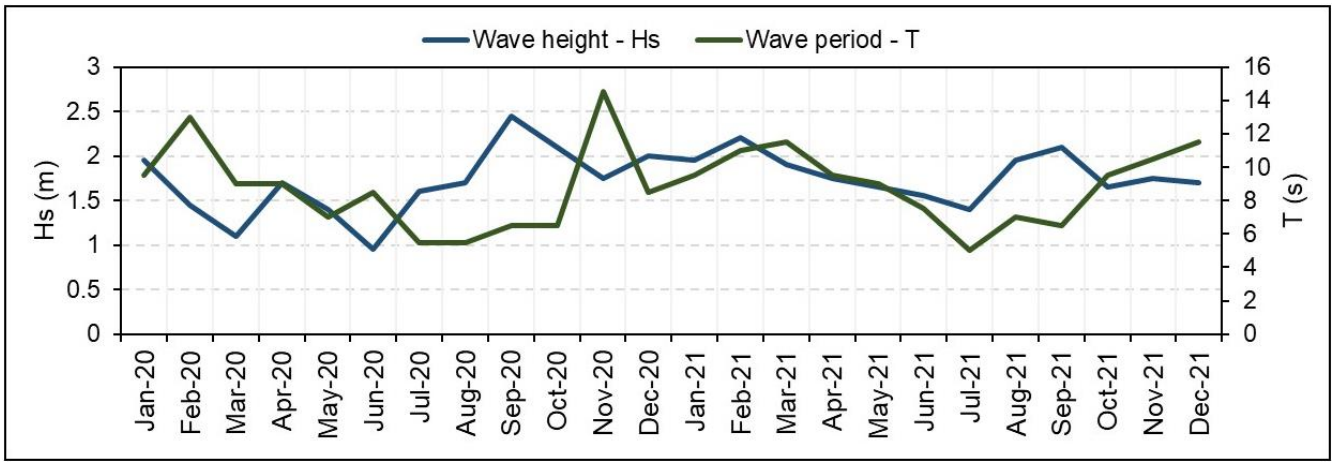

Figure 17. Significant wave height and period data from the Wavewatch III global model. Source: Surfguru.

Another factor not yet much explored that possibly interferes in the sediment dynamics, even if minimal in the beaches of the Brazilian Northeast, is the second-order flow results of the neotectonics where regions with faults that are targets of microseismic occurrence (SOUZA et al., 2005) Peroba and Redonda beaches are located in an area between duly mapped faults. Not being the study objective of this work, it is suggested that the following researchers analyze the possible contribution of the neotectonics in the coastal erosive or depositional processes in the area because the accurate understanding of the present tectonism is of extreme importance for studies that aim the definition of coastal evolutionary models.

This study joins the others in data validation using aerophotogrammetry techniques with RPA and the respective processing through the SfM algorithm in generating affordable DEMs and Orthomosaics of high-resolution images. On the other hand, the results will serve as an alternative tool for the coastal management of the municipality of Icapuí.

6. Conclusions

The results of this research were based on the survey of photogrammetric data with RPA on the beaches of Peroba and Redonda, which proved to be extremely important in detecting morphological changes and calculating short-term sediment balance along the beaches. The resolution of the DEMs and orthophoto mosaics generated were 23 cm and 2.88 cm, respectively. This indicates that the high resolution of the product allowed the volume calculation and estimation of shoreline position change closer to reality.

The coastal coast of Icapuí is highly dynamic, presenting different erosion and deposition rates from beach to beach due to the tidal regime, wave, and human interventions. Between August 2020 and August 2021, Peroba Beach had a positive balance, resulting in a sediment gain estimated at 18,815 m^3. At Redonda Beach, the balance was negative, and the volume of sediment eroded was estimated at -1,230 m^3. In the same period, the average variation rate of the coastline at Peroba Beach was 0.87 m/year, representing stability. At Redonda Beach, the average mobility rate of the coastline was estimated at 1.27 m/year, representing a gentle degradation.

Sandy sediments characterized the beaches with fractions ranging from very fine to medium sand, pointing to very fine to fine sand. The medium grain of very fine sand is associated with the best selection and is concentrated immediately to the downdrift of the promontory that separates the two beaches, being able to conclude that this, in conjunction with the abrasion platform generated by the rocky outcrops, exerts a direct influence on the hydrodynamic processes that affect the wave and tidal currents in this portion, consequently changing these granulometric parameters.

Although the study was of short duration, it detected that the eastern portions of the beaches of Peroba and Redonda are the ones that most go through erosive processes. As a consequence, occurs the retraction of the

shoreline. These results cannot be seen as an erosion trend but rather as an occurrence since erosion can be attributed to the combination of rocky promontories, tidal currents, waves, and the low slope of the beaches. The deposition can be associated with the curvilinear characteristics, the rocky outcrops between Peroba and Redonda that act as abrasion platforms and make possible the retention of sediments transported by littoral drift from the east to the west coast, especially on the beach of Redonda, the currents. Erosion can be attributed to rocky headlands, tidal currents, waves, and low beach gradients. The stability of the coastline in localized stretches of Peroba Beach and the entire eastern and central stretch of Redonda Beach may be attributed to human actions due to the construction of coastal erosion containment works.

The method applied in this work can be replicated in other beaches of the Municipality of Icapuí as well as on any coast of the State of Ceará and Brazil to estimate the volumetric variation of sediment and the dynamics of transport in order to contribute as a source of information for the management of the vulnerability of coastal areas. With this in mind, it is recommended that monitoring be carried out over a more extended period with the RPAs in order to ascertain whether or not there are erosion trends.

Author's contributions: Chacanza: Conception of the initial project and methodological details, organization of the fieldwork, data processing and analysis, and writing of the article; Almeida and Freire: Revision of the article and supervision; Silva Neto: provision and piloting of the RPA and support in the fieldwork; Medeiros and Abreu Neto: Support in the fieldwork. All the authors have read and agreed to the published version of the manuscript.

Acknowledgments: The authors would like to thank the Conselho Nacional de Desenvolvimento Científico e Tecnológico (CNPq) and The Academy of Sciences for the Developing World (TWAS) for awarding the research grant under process No. 166322/2018-0, as well as the Coordenação de Aperfeiçoamento de Pessoal de Nível Superior (CAPES), the Postgraduate Program in Geology at the Federal University of Ceará, the Marine and Applied Geology Laboratory (LGMA), the Geoprocessing Laboratory of Ceará (GEOCE), and the Púnguè University (UniPúnguè), Mozambique.

Conflict of Interest: The authors declare not having any conflict of interest. The funders had no interference in the development of the study, in the collection, analysis, or data interpretation, in the writing of the manuscript, or in the decision to publish the results.

References

1. ALMEIDA, J.C.D.; ALBUQUERQUE, M.G.; ALVES, D.C.L.; ESPINOZA, J.M.A. Uso de aeronave remotamente pilotada (RPA) no estudo da geomorfometria de sangradouros: estudo de caso do balneário Cassino, RS. **Labomar – Arquivos de Ciências do Mar**. Fortaleza. 53(especial), p. 61-69. 2021. ISSN 0374-5686. DOI: 10.32360/acmar.v53,supl.,42680
2. ALBUQUERQUE, M.G.; Alves, D.C.L.; ESPINOZA, J.M.A.; OLIVEIRA U.R.; SIMÕES, R.S. 2018a. Determining shoreline response to meteo-oceanographic events using remote sensing and unmanned aerial vehicle (UAV): case study in southern Brazil. **Journal of Coastal Research**. Special Issue No. 85, p. 766–770, 2018a. Coconut Creek (Florida). ISSN 0749-0208.
3. ALBUQUERQUE, M.G.; ESPINOZA, J.M.A.; ALVES, D.C.L. Uso de geotecnologias no gerenciamento de riscos associados à ação de eventos meteorológicos de grande intensidade no extremo sul do Brasil. **Mares e Litorais; Perspetivas transdisciplinares – Tomo VII da Rede BRASPOR**. 2018b. Disponível no site: https://www.researchgate.net/profile/Deivid-Leal-Alves/publication/341827754. Acesso 05/04/2021.
4. BARROS, E.L. **Erosão Costeira no Litoral do Município de Icapuí-CE na Última Década: Causas, Consequências e Perspectivas Futuras**. Tese (Doutorado Ciências Marinhas Tropicais) – Programa de Pós-graduação em Ciências Marinhas Tropicais, Instituto de Ciências do Mar – LABOMAR, Universidade Federal do Ceará. Fortaleza. 2018. 254p.
5. BLANCHARD, S.D.; ROGAN, J.; WOODCOCK, D.W. Geomorphic Change Analysis Using ASTER and SRTM Digital Elevation Models in Central Massachusetts, USA. **GIScience & Remote Sensing**. 47:1, p. 1-24. 2010. DOI: 10.2747/1548-1603.47.1.1
6. BORETTO, G.M.; ROUZAUT, S.; CIOCCALE, M.; GORDILLO, S.; BENITEZ, Y. La estructura cortical del arco de las Antillas Menores estimada a partir de técnica de funciones receptoras. **Revista Mexicana de Ciencias Geológicas**, V. 35, n. 3. p. 291-306. 2018. DOI: 10.22201/cgeo.200072902e.2018.3.865

7. BRASINGTON, J.; LANGHAM, J., and RUMSBY, B. Methodological sensitivity of morphometric estimates of coarse fluvial sediment transport. **Geomorphology**, 53: p. 299-316, 2003. DOI: h10.1016/S0169-555X(02)00320-3
8. CASELLA, E.; ROVERE, A.; PEDRONCINI, A.; MUCERINO, L.; CASELLA, M.; CUSATI, L.A.; VACCHI, M.; FERRARI, M. and FIRPO, M. Study of wave runup using numerical models and low-altitude aerial photogrammetry: A tool for coastal management. **Estuarine, Coastal and Shelf Science**. 149, p. 160-167. 2014. DOI: 10.1016/j.ecss.2014.08.012
9. CHACANZA, M.S.; ALMEIDA, N.M.; FREIRE, G.S.S; SILVA NETO, C.A.; ABREU NETO, J.C.; JALANE, O.I. 2022. Análise da Variação da Linha de Costa no Trecho Entre as Praias de Peroba e Redonda no Município de Icapuí-Ceará, Brasil, a Partir de Imagens de Satélite Aplicando o DSAS. São Paulo. UNESP. Geociências. v.41, n.4, p.377–396. ISSN:1980-900X. DOI: https://doi.org/10.5016/geociencias.v41i04.16718
10. CHEN, B.; YANG, Y.; WEN, H.; RUAN, H.; ZHOU, Z.; LUO, K.; ZHONG, F. High-resolution monitoring of – Beach topography and its change using unmanned aerial vehicle imagery. **Ocean and Coastal Management**, 160, 103-116, 2018. 0964-5691. DOI: 10.1016/j.ocecoaman.2018.04.007
11. COSTA, L.R.F.G. **Geotecnologias aplicadas ao monitoramento da cobertura sedimentar do litoral de Icapuí (Ceará) entre 1985 e 2018**. Tese (Doutorado em Geologia) – Programa de Pós-graduação em Geologia, Universidade Federal do Ceará. Fortaleza. 2019. 143p.
12. COSTA, S.; COELHO, C., 2013. Northwest coast of Portugal – Past behavior and future coastal defense options. **Journal of Coastal Research**. Special Issue No. 65, p. 921-926. ISSN 0749-0208.
13. COWELL, P.J.; THOM, B.J. Morphodynamic of coastal evolution. In: CARTER, R.W.G.; WOODROFFE, C.D. (Ed.). **Coastal Evolution: Late Quaternary shoreline morphodynamics**. Cambridge. Cambridge University Press. (2), p. 33-59. 1994. ISBN 0-521-41976 X
14. DAI, W.Q.; LI, H.; ZHOU, Z.; CYBELE, S.; LU, C.Z.; ZHAO, K.; ZHANG, X.Y.; YANG, H.T.; LI, D.Y. 2018. UAV Photogrammetry for Elevation Monitoring of Intertidal Mudflats. **Journal of Coastal Research**. Special Issue No. 85, pp. 236-240. Coconut Creek (Florida), ISSN 0749-0208
15. DEL RÍO, L.; GRACIA, F.J.; BENAVENTE, J. 2016. Multiple-source cliff erosion in Southern Spain: current risk and future perspectives. **Journal of Coastal Research**. Special Issue. No. 75; pp. 1072 - 1077. Coconut Creek (Florida). ISSN 0749-0208.
16. EICHMANNS, C.; SCHÜTTRUMPF, H. Influence of Sand Trapping Fances on Dune Toe Growth and Its Relation with Potential Aeolian Sediment Transport. **Journal of Marine Science and Engineering**. 9, 850. 2021. DOI: 10.3390/jmse9080850
17. FOLK, R.L.; WARD, W.C. Brazos river bar: a study in the significance of grain size parameters. **Journal of Sedimentary Petrology**. Vol. 27. No. 1. p. 3-26. 1957.
18. GOVAERE, G.; VIQUEZ, R.; ALFARO, H. Use of Drone Technology and Photogrammetry for Beach Morphodynamics and Breakwater Monitoring. Proccedings of the 6th International Conference on the Application of Physical Modelling in Coastal and Port Engineering and Science (Coastlab16). May, 2016. Canada. **Anais**… Ottawa. p. 10-13. 2016.
19. GRIGGS, G.; PATSCH, K. The protection/hardening of California's coast: Times are changing. **Journal of Coastal Research**. 00(0), 000–000. 2019. Coconut Creek (Florida), ISSN 0749-0208.
20. HIMMELSTOSS, E.A.; HENDERSON, R. E.; KRATZMANN, M.G.; FARRIS, A.S. 2018. Digital Shoreline Analysis System (DSAS) version 5.0 user guide: U.S. Geological Survey Open-File Report, 2018–1179, 110p. DOI: 10.3133/ofr20181179
21. IPECE – Instituto de Pesquisa e Estratégia Econômica do Ceará. Ceará em Números. **Caraterização Territorial**. Fortaleza, 2007. Disponível em: http://www.ipece.ce.gov.br/publicacoes/ceara_em_numeros/2008/infra/. Acesso 03/06/2019.
22. JANUŠAITĖ, R.; KARALIŪNAS, V.; BEVAINIS, L. Application of Remote Sensing Methods in Research of Nearshore Sandbars, Curonian Spit, Lithuania. **Baltic J. Modern Computing**, Vol. 7. 2019. DOI: 10.22364/bjmc.2019.7.4.08
23. JAUD, M.; DELACOURT, C.; DANTEC, N.L.; ALLEMAND, P.; AMMANN, J.; GRANDJEAN, P.; NOUAILLE, H.; PRUNIER, C.; CUQ, V.; AUGEREAU, E.; COCQUEMPOT, L.; FLOC'H, F. Diachronic UAV Photogrammetry of a Sandy Beach in Brittany (France) for a Long-Term Coastal Observatory. **International Journal of Geo-Information**. 2019. DOI: 10.3390/ijgi8060267

24. JAUD, M.; BERTIN, S.; BEAUVERGER, M.; AUGEREAU, E.; DELACOURT, C. RTK GNSS-Assisted Terrestrial SfM Photogrammetry without GCP: Application to Coastal Morphodynamics Monitoring. **Remote Sens**. 12, 1889. 2020. DOI: 10.3390/rs12111889
25. JAYSON-QUASHIGAH, P-N.; APPEANING ADDO, K. and KUFOGBE, S.K. Shoreline monitoring using medium resolution satellite imagery, a case study of the eastern coast of Ghana. **Journal of Coastal Research**. Special Issue No. 65, p. 511-516; 2013. ISSN 0749-0208. DOI: 10.2112/SI65-087.1
26. JAYSON-QUASHIGAH, P-N.; APPEANING ADDO, K.; AMISIGO, B.; WIAFE, G. Assessment of short-term beach sediment change in the Volta Delta coast in Ghana using data from Unmanned Aerial Vehicles (Drone). **Ocean and Coastal Management**. 2019. DOI: 10.1016/j.ocecoaman.2019.104952
27. KALIRAJ, S; CHANDRASEKAR, N.; RAMACHANDRAN, K.K. Mapping of coastal landforms and volumetric change analysis in the south west coast of Kanyakumari, South India using remote sensing and GIS techniques. **The Egyptian Journal of Remote Sensing and Space Science**. 20, p. 265-282. 2017. DOI: 10.1016/j.ejrs.2016.12.006
28. KIM, C.H.; KIM, H.W.; PARK, C.H.; KIM, W.H.; LEE, M.H.; CHOI, S.Y.; DO, J.D. Coastline change measurement using shipborne mobile LiDAR in Anmok Beach, Gangneung, Korea. **Journal of Coastal Research**. Special Issue. No. 85; pp. 601–605. 2018. Coconut Creek (Florida). ISSN 0749-0208. DOI: 10.2112/SI85-121.1
29. LAPORTE-FAURET, Q.; MARIEU, V.; CASTELLE, B.; MICHALET, R.; BUJAN, A.; ROSEBERRY, D. Low-Cost UAV for High-Resolution and Large-Scale Coastal Dune Change Monitoring Using Photogrammetry. **Journal of Marine Science and Engineering**, 7. 63. 2019. DOI: 10.3390/jmse7030063
30. LANE, S.N.; WESTAWAY, R.M.; HICKS, D.M. Estimation of Erosion and Deposition Volumes in a Large, Gravel-Bed, Braided River Using Synoptic Remote Sensing. **Earth Surface Processes and Landforms**, 28, p. 249-271. 2003. DOI: 10.1002/esp.483
31. MARTINS, L.R. Análise Recente de Sedimentos e Tamanho de Grão. **Gravel**. Porto Alegre. No. 2. p. 40-56. 2003. ISSN 1678-5975.
32. MASSELINK, G.; CASTELLE, B.; SCOTT, T.; DODET, G.; SUANEZ, S.; JACKSON, D.; FLOC'H, F. Extreme wave activity during 2013/2014 winter and morphological impacts along the Atlantic coast of Europe. **Geophysical Research Letters**. 43(5). p. 2135-2143. 2016. DOI: 10.1002/2015GL067492
33. MCLAREN, P.; BOWLES, D. The effects of sediment transport on grain-sise distributions. 1985. **Journal of Sedimentary Petrology**. Vol. 55, No. 4. p. 0457-0447.
34. MEIRELES, A. J. A.; SANTOS, A.M.F. **Atlas de Icapuí - CE**. Projeto de Olho na Água. 1a Edição. Fortaleza. Editora Fundação Brasil Cidadão, 2012. 156p.
35. MMA – Ministério do Meio Ambiente. **Plano Nacional de Gerenciamento Costeiro (PNGC II)**. Brasília-DF. (s.d.). Disponível em: https://www.mma.gov.br/estruturas/sqa_sigercom/_arquivos/pngc2_78.pdf. Acesso 12/09/2019.
36. MUEHE, D. 2013. Erosão costeira, mudança do clima e vulnerabilidade. In: GUERRA, A.J.T.; JORGE, M.C.O. (Ed.). **Processos erosivos e recuperação de áreas degradadas**. São Paulo. Oficina de Textos. 161-186p. ISBN 978-85-7975-079-3
37. NAGDEE, M.R.M.S.; NURSE, L.; INNISS, L.; CHADWICK, A.; JOHNSON, T. Historical shoreline mapping: Application of the Digital Shoreline Analysis System to the evolution of Worthing Beach, Barbados, following Hurricanes Allen (1980) and Ivan (2004). **Journal of Coastal Research**. 36(2), p. 313-318. 2020. Coconut Creek (Florida). ISSN 0749-0208.
38. NORDSTROM, K.F., **Recuperação de Praias e dunas**. São Paulo. Oficina de Textos. 2010. 263p. ISBN 978-85-7975-006-9.
39. PAGÁN, J.I.; BAÑÓN, L.; LÓPEZ, I.; BAÑÓN, C.; ARAGONÉS, L. Monitoring the dune-beach system of Guardamar del Segura (Spain) using UAV, SfM and GIS techniques. **Science of the Total Environment**, 687, p. 1034-1045. 2019. ISSN 0048–9697. DOI: 10.1016/j.scitotenv.2019.06.186
40. PINHEIRO, L.d.S.; MORAIS, J.O. de; MAIA, L.P. The Beaches of Ceará. In: SHORT, A.D.; KLEIN, A.H. da F. (Ed.). Brazilian Beach Systems. **Coastal Research Library**. p. 175-199. 2016. DOI: 10.1007/978-3-319-30394-9_7
41. PITMAN, S.J.; HART, D.E.; KATURJI, M.H. Application of UAV techniques to expand beach research possibilities: A case study of coarse clastic beach cusps. **Continental Shelf Research**. 184, p. 44-53. 2019. 0278–4343. 10.1016/j.csr.2019.07.008

42. PORTELA, J.P.; FREIRE, G.S.S.; MORAES, M.V.A.R.; SILVA, C.A. Evolução da Morfologia Costeira do Litoral Oeste de Icapuí-CE. **Revista Geonorte**. Edição Especial 4, V.10, N.1, p. 89-93, 2014. ISSN 2237-1419.
43. QI, F.; WU, X.; WANG, Z.; WANG, C.; DUAN, H.; LIU, M.; XU, J. Transport and deposition processes of the sediment depocenter off the Shandong Peninsula: An observational study. **Continental Shelf Research**. 244, 104763. 2022. ISSN 0278–4343. DOI: 10.1016/j.csr.2022.104763
44. SILVA, R.V.M.; AGUIAR, L.S.; MAIA, J.L.A.; LIMA, M.Z.C. Uso de veículos aéreos não tripulados nos estudos da zona costeira no litoral sul do Rio Grande do Norte, Brasil. XVIII Simpósio Brasileiro de Geografia Física Aplicada. Universidade Federal do Ceará. **Anais**... Fortaleza-CE. 11 a 15 de Junho de 2019.
45. SILVA NETO, C.A.; DUARTE, C.R.; SOUTO, M.V.S.; FREIRES, E.V.; SOUSA, W.R.N.; SILVA, M.T. Caracterização dos setores erosivos e deposicionais da linha de costa de Icapuí (CE) com base em produtos de sensoriamento remoto e técnicas de geoprocessamento. **Revista Brasileira de Geografia Física**. v.13, n. 01. 143-155. 2020.
46. SMITH, M.W.; CARRIVICK, J.L.; QUICEY, D.J. Structure from motion photogrammetry in physical geography. **Progress in Physical Geography**, 40, p. 247-275. 2015. DOI: 10.1177/0309133315615805
47. SIMÕES, R.S.; OLIVEIRA, U.R. Monitoramento mensal da linha de costa no Balneário Mostardense – RS entre 2016/2017 utilizando dados de VANT. **Quaternary and Environmental Geosciences**. 11(1): 1-18. 2020.
48. SOUZA, C.R.G.; SUGUIO, K.; OLIVEIRA, A.M.S.; OLIVEIRA, P.E. (Ed.). **Quaternário do Brasil**. 1a ed. ABEQUA. Ribeirão Preto/SP. pp. 382. 2005. ISBN 85-86699-47-0.
49. SUGUIO, K. **Geologia Sedimentar**. 1a ed. Blucher. São Paulo. 2003. 11-42p.
50. SUGUIO, K. Geologia do Quaternário e mudanças ambientais. Oficinas de Textos. São Paulo. 2010. 408p.
51. TAAOUATI, M.; EL MRINI, A.; NACHITE, D. Beach Morphology and Sediment Budget Variability Based on High Quality Digital Elevation Models Derived from Field Data Sets. **International Journal of Geosciences**. 2, 111-119. 2011. DOI: 10.4236/ijg.2011.22012
52. WENTWORTH, C.H. A scale of grade and depositional processes. **Journal of Geology**. 30, p. 377-392. 1922.
53. WHEATON, J.M.; BRASINGTON, J.; DARBY, S.E.; SEAR, D.A. Accounting for uncertainty in DEMs from repeat topographic surveys: improved sediment budgets. **Earth Surf. Process. Landforms**, 35, p. 136-156. 2010. DOI: 10.1002/esp.1886.